Riset Geologi dan Pertambangan
(Geology and Mining Research)

RESEARCH ARTICLE
OPEN ACCESS

Riset Geologi dan Pertambangan (2025) Vol. 35, No. 2, 109–130
DOI: 10.55981/risetgeotam.2025.1397

Keywords:
Karaha
Sadakeling
Volcanostratigraphy
Hazards
Risk

Corresponding author:
Willi F.S. Banggur
wilf001@brin.co.id

Article history:
Received: 05 May 2025
Revised: 07 0ctober 2025
Accepted: 14 October 2025

Author Contributions:
Conceptualization: WFSB, MNK
Data curation: WFSB, MNK
Formal analysis: WFSB, MNK, MA
Funding acquisition: WFSB, MNK Investigation: WFSB, MNK
Methodology: WFSB, MA, MNK, AEPM
Supervision: WFSB, MNK, AEPM, MZT
Visualization: WFSB
Writing – original draft: WFSB
Writing – review & editing: WFSB, MZT, FN

Citation:
Banggur, W.F.S., Tuakia, M.Z., Abdurrachman, M., Kartadinata, M.N., Novico, F., Muhammad, A.E.P., Patria, C., 2025. Volcanostratigraphy and Geological Hazard Potential of the Karaha-Sadakeling Volcano Complex, West Java. *Riset Geologi dan Pertambangan, 35 (2)*, 109–130, doi: 10.55981/risetgeotam.2025.1397

Volcanostratigraphy and geological hazard potential of the Karaha-Sadakeling volcano complex, West Java, Indonesia

Wilfridus F.S. Banggur[1], Muhammad Zain Tuakia[2], Mirzam Abdurrachman[3], Muhammad Nugraha Kartadinata[4], Azrie E.P. Muhammad[3], Franto Novico[1], Cahya Patria[1]

[1]Research Center for Geological Disaster, National Research and Innovation Agency (BRIN), Bandung 40135, Indonesia
[2]Research Center for Geological Resources, National Research and Innovation Agency (BRIN), Bandung 40135, Indonesia
[3]Geological Engineering Department, Institut Teknologi Bandung, Bandung 40132, Indonesia
[4]Center for Volcanology and Geological Hazard Mitigation, Geological Agency, Bandung 40122, Indonesia

Abstract

The purpose of this study is to determine the type and distribution of volcanic rocks both laterally and vertically and to analyze the potential hazards of the Karaha-Sadakeling Volcanic Complex. Volcanostratigraphically, the volcanic evolution from old to young is Cakrabuana Crown, Sadakeling Crown, Ewaranda Crown, and Talagabodas Crown. The recognizable landforms are crater traces, volcanic cones, lava flow ridges, and alluvial plains. The north-south oriented volcanic cone morphology of the study area parallels an approximate major fault that passes between the Cakrabuana Complex to the northeast, and the Karaha-Sadakeling Complex. The northern part is dominated by Sadakeling Crown volcanic deposits, the central part is composed of Ewaranda Crown deposits, and the southern part is dominated by Talagabodas deposits. The magmatic evolution shows the process of magma assimilation and mixing with primitive magma. Potential volcanic disasters can include pyroclastic fall, pyroclastic flows, and lava flows. Primary eruptions are inferred to originate from Karaha Crater, which exhibits ongoing volcanic activity.

1. Introduction

Understanding volcanostratigraphy and potential geological hazards is an important aspect of disaster mitigation efforts in volcano areas. Identifying the types of volcanic hazards and estimating the potentially affected areas allows for more effective mitigation measures, including evacuation planning and risk reduction for populations living around volcanoes. By understanding the eruption patterns and geological characteristics of a volcano complex, disaster risk can be minimized (Bronto et al., 2016; Groppelli and Molist, 2013; Keskin et al., 1998; Lockwood and Hazlett, 2013; Petterson and Treloar, 2004; Tilling, 1989; Tsai et al., 2010).

Mount Karaha-Sadakeling, located in Tasikmalaya Regency, Indonesia (Figure 1), constitutes a volcanic complex characterized by a ridge of hills that extends northward from Mount

Galunggung, with elevations ranging from 500 to 1,676 meters (Bronto, 1989). The geothermal resources within this complex are derived from quartz diorite intrusions at a depth of approximately 1,500 meters, featuring two primary zones: Karaha in the north and Talagabodas in the south, each possessing distinct geothermal systems (Arisbaya et al., 2018; Danakusumah and Suryantini, 2020; Moore et al., 2002).

In the southern region, a comprehensive volcanostratigraphic analysis of the Galunggung-Talagabodas complex delineates the sequence of rock formations from oldest to youngest, which includes the Cakrabuana Crown, Sadakeling Crown, Sawal Crown, Talagabodas Crown, and Galunggung Crown (Budhitrisna, 1986; Ramadhan et al., 2016). Pertamina (1990) in Irada (2017) provides a regional overview encompassing Mount Galunggung in the south to Cakrabuana in the north, detailing that the stratigraphy of Karaha Bodas is arranged from oldest to youngest as follows: Cakrabuana pyroclastic breccia, Sadakeling pyroclastic breccia, Telaga Bodas pyroclastic deposits, Telaga Bodas andesitic breccia, Ewaranda pyroclastic breccia, Ewaranda andesite, Putri tuff, and alluvial deposits. This study does not present detailed data on each volcanic product from the various Crowns within the study area. Subsequently, Muhammad et al. (2025) classified the volcanic rocks in the study area from oldest to youngest, identifying the Cakrabuana Crown, Sadakeling, Karaha Crown, and Talagabodas Crown (Figure 2).

The geochemical characteristics of rocks from the Karaha and Talagabodas Complexes suggest a complex magmatic evolution, closely associated with magma differentiation, tectonic settings, and the potential for geothermal systems (Muhammad et al., 2025; Kausar et al., 2016, 2024). Nevertheless, those studies have not fully addressed questions concerning the detailed stratigraphic relationships between each volcano and its eruptive products, as well as their associated hazard potential, remaining limited in scope regarding the geothermal potential of the Karaha-Sadakeling Volcanic Complex. In this study, we focus on identification of types of the erupted rocks, their vertical and lateral delineations, the origin and formation process, and analyzing the potential geological hazards from the volcanic aspect. Analysis of potential volcanic hazards is carried out based on volcanostratigraphic relationships and field observations in the form of surface manifestations of volcanic activity.

2. Geologic setting

The study area is physiographically located within the Quaternary mountain zone (van Bemmelen, 1949). The Cretaceous subduction zone in Java is recognized to have originated in the Ciletuh region, extending through the Papandayan Volcanic Complex in southern West Java, passing the Lok Ulo area in Central Java, and continuing further northward Surabaya in the eastern part of the island (Abdurrachman, 2012; Katili, 1975; Figure 1a).

According to Alzwar et al. (1992) and Katili and Sudradjat (1984), the southern area of the Bandung Basin belongs to a Quaternary volcanic group located between three major fault boundaries. In the northwest, there is the Sukabumi-Padalarang left-dipping fault zone, while in the northeast there is the Cilacap-Kuningan right-dipping fault zone. In the south, there is a normal fault bordering the Southern Mountains. Regionally, the oldest rocks in the South Bandung area are Miocene-aged andesitic lavas (Bronto and Koswara, 2006). Then according to Haryanto (2006; 2013) and Haryanto et al. (2018), the Karaha-Sadakeling Complex research area is part of a north-south oriented volcano distribution pattern influenced by regional structures with the same north-south direction. Tectonic activity is influential in shaping the pattern of geological structures and causing landscape asymmetry, which shows the interaction between tectonics and volcanism regionally.

Based on the Geological Map of Tasikmalaya Sheet by Budhitrisna (1986), the rocks in the study area are composed of Quaternary volcanic products in the form of breccias, tuffs, and lava flows, which are aligned above the Tertiary volcanic andesitic lava rocks, and the geological structure pattern shows a northwest-southeast direction that passes Mount Cakrabuana in the east and Mount Sadakeling in the west. Local faults in the Karaha-Sadakeling complex also follow this alignment pattern. The Karaha-Sadakeling volcanic

complex is part of the Tertiary magmatic arc located on a volcanic front based on the depth of the Benioff Zone (Sendjaja et al., 2009; Soeria-Atmadja et al., 1994).

Rock geochemical analysis of 9 rock samples from the total rock samples in this study has been conducted (see Table 1 in Muhammad et al., (2025)) and shows that the characteristics of basaltic-andesitic magmas with sub-alkaline properties, as well as magma contamination are thought to originate from the interaction between the Sundaland crust in the north and Gondwana in the south, with trace elements (Sr and Nd) similar to Southeast Australian granites.

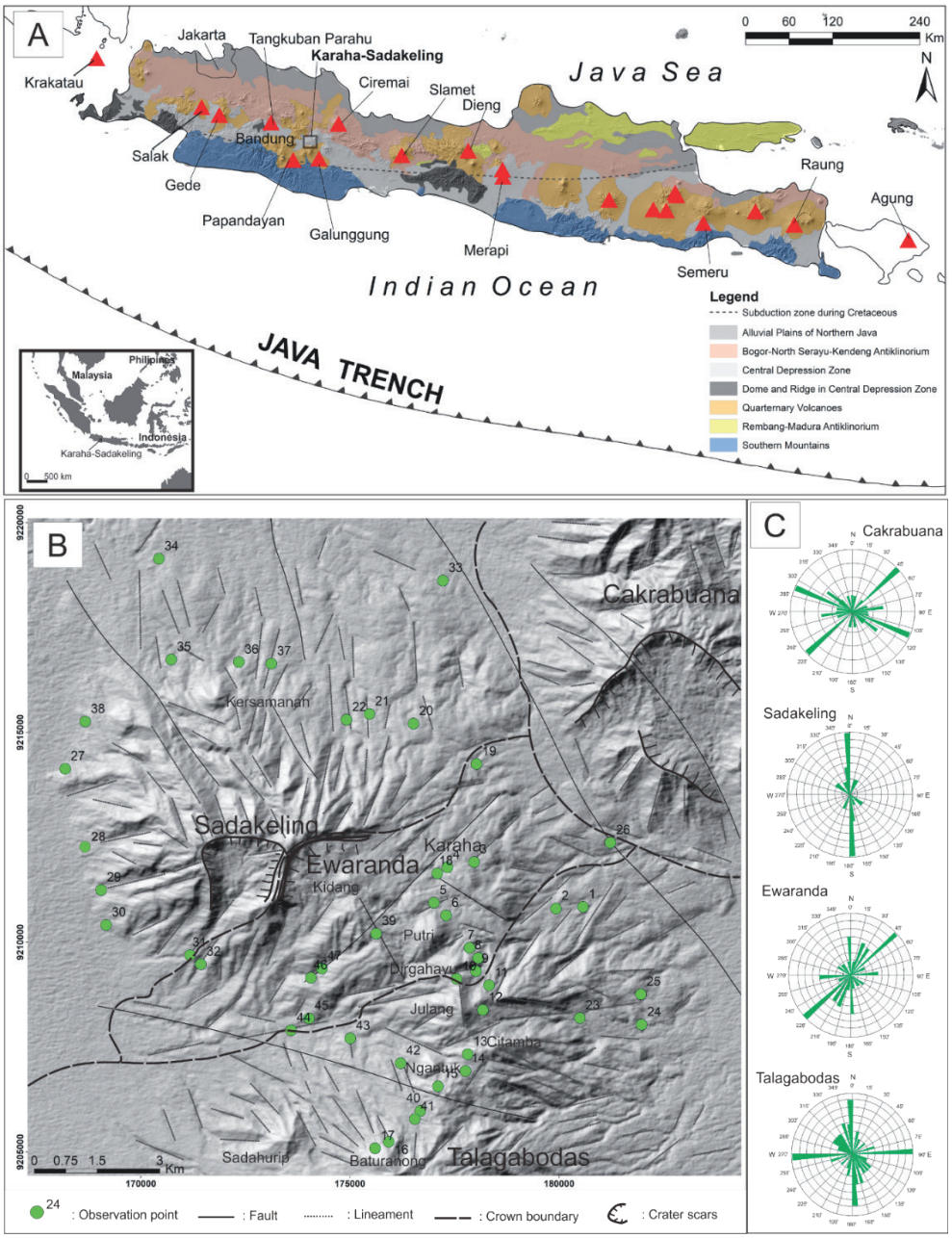

Figure 1. a) Physiographic map of Java Island exhibits the study area situated in the Quaternary volcanoes zone (Bemmelen, 1970). The thin gray dotted line indicates the trace of the subduction zone during the Cretaceous period (Katili, 1975). b) The DEM of Karaha-Sadakeling volcanic complex shows field observation points marked by small green circles, the boundary between Crowns marked by thick black dotted lines, fault lines marked by black lines, and lineament lines marked by gray dotted lines. c) The Rosset diagrams each Khuluk represents the morphological shape of lava flow ridges and valleys.

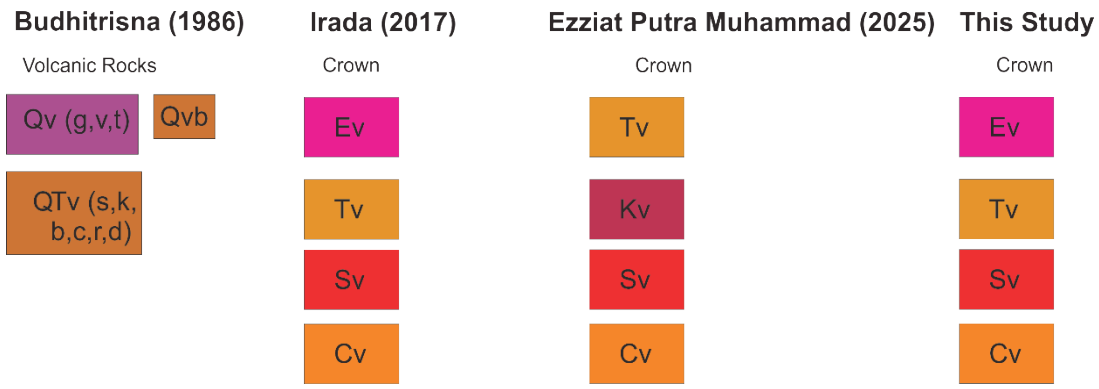

Figure 2. Comparison of the stratigraphic columns of the study area. Budhitrisna (1986) categorized the volcanic rocks regionally into older volcanic products (QTv), which include Mount Sawal, Mount Kukus, Mount Cakrabuana, Mount Sadakeling, Mount Cereme, and Mount Cikuray, and younger volcanic products (Qv), which comprise Mount Galunggung, Mount Talagabodas, and Mount Cereme. Pertamina (1990) in Irada (2017) conducted a regional mapping of each crown; however, detailed delineation of each Khuluk product has yet to be accomplished. The chronological sequence from oldest to youngest is as follows: Mount Cakrabuana, Mount Sadakeling, Mount Ewaranda, and Mount Talagabodas. Muhammad et al. (2025) have mapped the volcanostratigraphic aspects of the study area and performed geochemical analyses of the rocks; however, the differentiation in the delineation and eruption sources of the products from Sadakeling, Ewaranda and Talagabodas still requires further refinement. Abbreviations: Tv: Talagabodas volcanic, Ev: Ewaranda volcanic, Sv: Sadakeling volcanic, Cv: Cakrabuana volcanic.

3. Data and methods

This study follows the volcanostratigraphic classification of the Indonesian Stratigraphic Code by Martodjojo and Djuhaeni (1996), which consists of Arc (a series of volcanoes with similar tectonic settings), Bregada (deposits from two or more Crowns, often associated with calderas), Crown or Khuluk in Indonesian terminology (deposits from one or more eruption points that form the body of the volcano), and Hummock or Gumuk in Indonesian terminology (parts or products of Crown formed by central or lateral eruptions).

The distribution of volcanic products was analyzed using the national digital elevation model (DEMNAS) satellite imagery to determine the source of the eruption and the distribution of rocks based on the volcanostratigraphic method. The DEMNAS by Badan Informasi Geospasial (2018) was built using IFSAR and TERRASAR-X data (5 m), ALOS PALSAR data (11.25 m), and masspoint data from stereo-plotting, with a spatial resolution of 0.27 arcseconds and referenced to the EGM2008 vertical datum (Figure 1b).

The Crown boundary follows the morphological pattern formed by a collection of volcanic deposits that still have or had the same source of eruption, forming a volcanic body. The Crown boundary also takes into account the lateral or spread and projection boundaries of the volcanic material (Bronto et al., 2016), and the type of rocks is verified by conducting field checks.

A total of 47 observation stations from the Karaha-Sadakeling Volcano Complex were collected (Figure 1b), with 33 samples were analyzed petrographically for mineral composition, rocks texture, and plagioclase microtexture representing each lava product from each Crowns in the Center for Volcanology and Geological Hazard Mitigation (CVGHM), Geological Agency. In addition, 5 observation points of pyroclastic outcrops and the 9 observations rest were morphological observations.

Analysis of alignment and structure using shaded digital elevation model (DEM) maps with azimuths of 0°, 45°, 60°, and 135° to obtain general alignment patterns in the study area (Figure 1b and c). Volcanostratigraphic relationship analysis was carried out for volcano hazard analysis which was then combined with the results of field condition observations to create a map of potential volcanic eruption hazards at the Karaha-Sadakeling Volcano Complex.

4. Results

Volcanic Landscape

Landscape analysis using DEM data, contour patterns, and field observations revealed 4 recognizable landforms, namely volcanic cones, volcanic craters, lava flow ridges, and alluvial plains. The volcanic cone morphology from north to south in the study area is Mount Kersamanah in the north, Mount Kidang, Mount Putri, Mount Dirgahayu, Mount Julang, Mount Citamba, Mount Ngantuk, Mount Baturahong, and Mount Sadahurip in the south. The morphology of volcanic craters recognized are Cakrabuana Crater in the northeast of the study area, Ewaranda Crater which is characterized by the avalanche of the crater wall, with an opening towards the southeast, and Sadakeling Crater which opens towards the southwest.

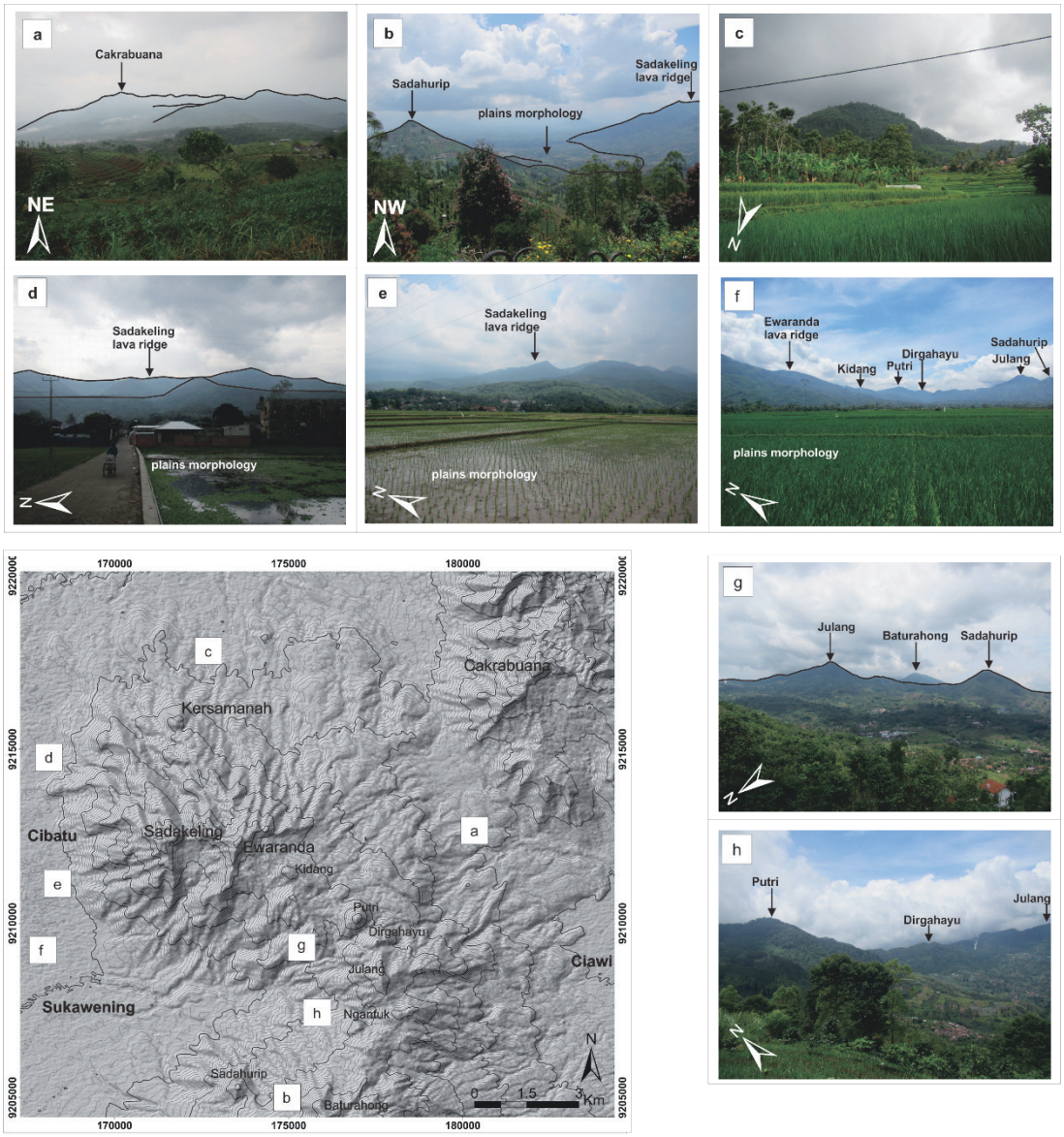

Figure 3. The Morphology of the Karaha-Sadakeling Volcanic Complex**.** The northeastern section is formed by the volcanic products of Cakrabuana (Photo 3a). The northwestern part exhibits the morphological characteristics of the volcanic products from Sadakeling. The central area is comprised of volcanic products from Ewaranda, while the southern section is constituted by the volcanic products of Talagabodas. Photo 3b, taken from the southernmost point of the study area, is closer to the position of the Sadahurip Volcanic Cone located to the south of the research area. At this vantage point, the photograph is oriented towards the northwest, showcasing the Sadahurip cone in the southern part, the plateau on the western side of Sadakeling (representing the location of photo points e and f), and the western flank of the Sadakeling lava flow ridge. Photos 3d, e, and f depict the lava flow ridge of Sadakeling to the west, and Ewaranda to the south of Sadakeling. The photographs were captured from the plateau in the western region of Sadakeling. In photo f, the orientation is relatively towards the east-southeast, displaying the lava flow ridge of Ewaranda, as well as Mount Kidang, Mount Putri, Mount Dirgahayu, Mount Julang, and Mount Sadahurip. Photo 3g illustrates Mount Julang and Mount Sadahurip with Mount Baturahong in the background, photographed relatively towards the south. Photo 3h shows Mount Putri, Mount Dirgahayu, and Mount Julang.

The volcanic landscape in the northeastern part of the study area is composed of volcanic products from the Cakrabuana Crown (Figure 3a). The Sadakeling Crown dominates the morphology in the northern, northwestern, and western sectors of the study area (Figure 3c, d, and e). Observation point 3b illustrates Mount Sadahurip, the southernmost volcanic cone of the study area and part of the Talagabodas Crown (visible in the left section of Figure 3b), the plain morphology (center of Figure 3b), and the ridge of Sadakeling lava flows located in the northern sector (right section of Figure 3b). Observation point 3c highlights the Kersamanah Mount in the northern part of the study area. Observation points 3d–f and h reveal lava flow ridges, the Sadakeling volcanic crater, and several volcanic cones in southern Ewaranda, including Mount Kidang, Mount Putri, Mount Dirgahayu, and Mount Julang. The southernmost margin of the study area is shaped by the Talagabodas Crown, which is characterized by distinct volcanic landforms such as the Sadahurip cone, Mount Julang, and Mount Baturahong (Figure 3g).

Lineament and Fault

Based on map interpretation using DEM shading method and contour patterns, the geological structures developed in the Karaha-Sadakeling Complex area include crater structures (circular), lineations, and faults (Figure 1b). Crater structures are found in Cakrabuana, Sadakeling, and Ewaranda. The alignments are generally north-south and southwest-northeast oriented (Figure 1c), with the main fault line located between the Cakrabuana Complex and the Karaha-Sadakeling Complex, passing through the Malangbong area to the southeast. In the Cakrabuana Complex, right inside the crater, it is estimated that there is a fault that is interpreted as a shift in the morphology of the Cakrabuana crater (Figure 1b). The crater structure which is a circular shape on the hilly morphology or top of a morphology is interpreted as a crater structure, which is found in Cakrabuana, Sadakeling and Ewaranda. There are also morphological forms that resemble cones, which are interpreted as volcanic cones including Kersamanah Cone part of Sadakeling Crown, Kidang Cone, Putri Cone and Dirgahayu Cone part of Ewaranda Crown, and Julang Cone, Ngantuk Cone, Sadahurip Cone and Baturahong Cone which are part of Talagabodas Crown.

Volcanic Deposits

Based on the lithologies exposed at the surface, the eruption products of the Karaha-Sadakeling Complex consist of lava flows, pyroclastic flows, pyroclastic falls, and laharic deposits. The northern part is dominated by Sadakeling lava flows, the central part is dominated by Ewaranda pyroclastic flow deposits, and the southern part is dominated by Talagabodas pyroclastic fall deposits (see Figure 4 for the eruption products of each Crowns, and Figure 5 for the volcanostratigraphic map and column stratigraphy, and location type for each photo that mentioned in Figure 4). The volcanic stratigraphic map illustrates the spatial distribution of volcanic products, while the stratigraphic column provides an interpretation of the depositional sequence of each eruptive unit (Figure 5). Additionally, three cross-sections were constructed (Figure 6): 1. extending from the Sadakeling edifice in the northwest to the Talagabodas edifice in the southeast (A–B), 2. from Sadakeling in the west to Talagabodas in the east (C–D), and 3. from Talagabodas in the southeast to Cakrabuana in the northeast (E–F).

The Sadakeling edifice is subdivided into 15 hummocks, consisting of Sadakeling lava flows (Sl) labeled Sl1–Sl13, and pyroclastic flows categorized as Sadakeling pyroclastic flows (Sap), and one volcanic cone, namely the Kersamanah volcanic cone (Ksl). The pyroclastic flow deposits (Sap) form the oldest deposits that shape the morphology of the western plain (Figure 3e and f), and are estimated to extend as far as the Cimanuk River, located in the western part of the study area.

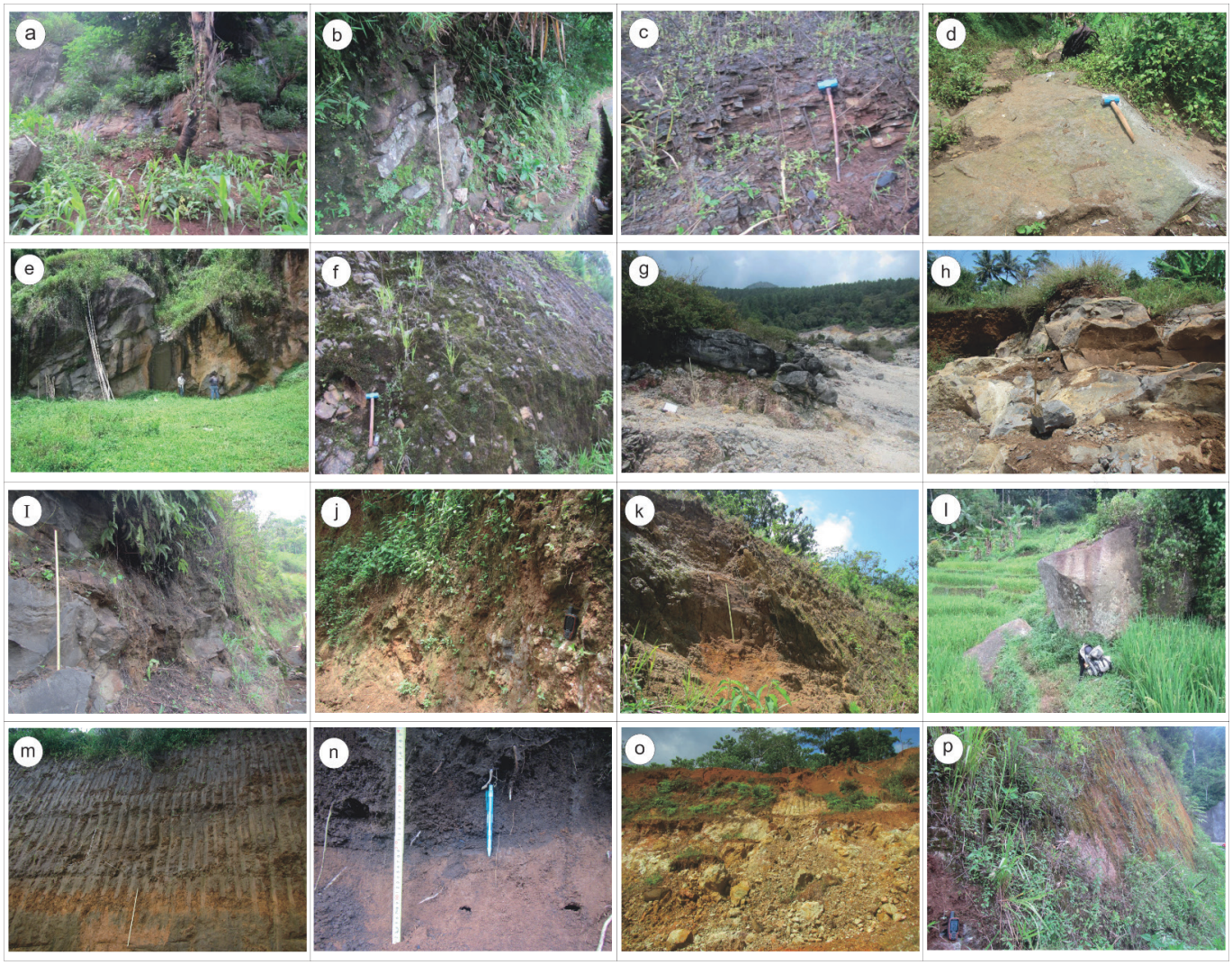

Figure 4. Sample photographs of rock types and their distribution in the Karaha-Sadakeling Complex. Photographs a-c, e, o, h, and j represent Sadakeling lava flow products. Photographs g, I, l, n, and p represent Ewaranda products, and d, f, k, and m represent Talagabodas products. See Figure 5 for the position of each photograph on the volcanostratigraphic map.

Sadakeling lava is primarily composed of andesitic to basaltic–andesitic lava flows (Table 1), which are distributed across the northern to western sectors of the study area (Figure 4a, b, c, e, h, j, and o). The oldest lava unit (Sl1) is exposed in the northwestern sector, particularly within the Cisalak quarry area (Figure 1b, station 34; Figure 4h), while progressively younger lava flows (Sl2–Sl5) occupy the northeastern sector (Figure 1b, stations 20–22, 33, and 37; Figure 4o and b). In the northern part, lava units Sl1, Sl6, and Sl7 are truncated by the intrusion of the Kersamanah Volcanic Cone (Figure 1b, stations 34–36; Figure 3c). The western sector is characterized by lava flows Sl9–Sl13 (Figure 1b stations 27, 29, 30-32, and 38; Figure 4a, c, and e). Within the Sadakeling crater, the volcanic depression is interpreted as a collapse structure (Sgv).

The Ewaranda edifice is mainly characterized by pyroclastic flow deposits and lava flows consisting of basalt-andesite rocks (Figure 4g, i, and l), with two volcanic cones located in the southern sector: Mount Putri, consisting of lava flows and pyroclastic fall deposits (Pjp) (Figure 1b station 39; Figure 4n), and Mount Dirgahayu, which mainly consists of lava flows (Figure 1b station 39; Figure 4p).

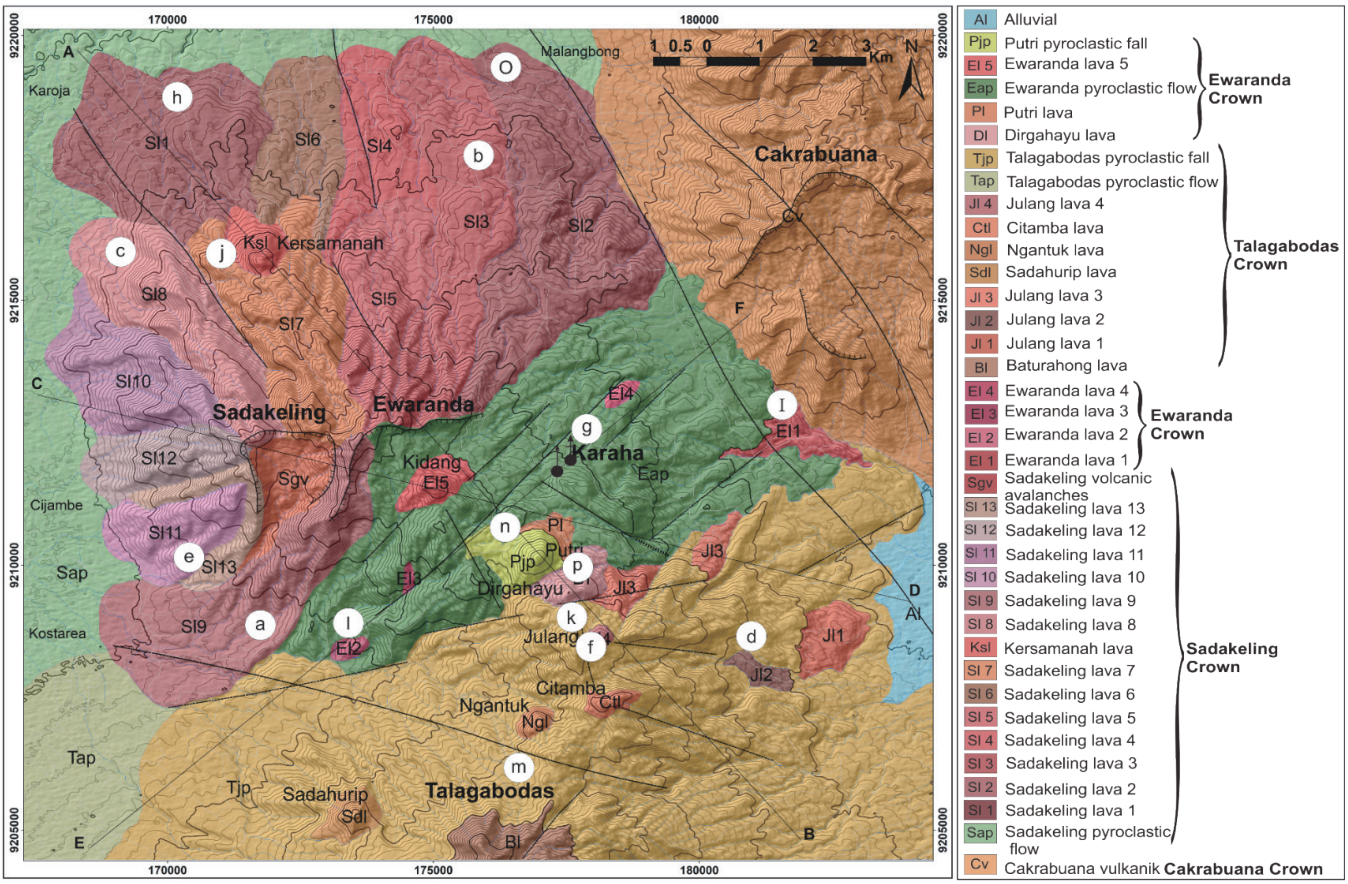

Figure 5. Volcanostratigraphy map and stratigraphy column of Karaha-Sadakeling Volcano Complex. See Figure 4 for detail rocks photos of alphabet on the map.

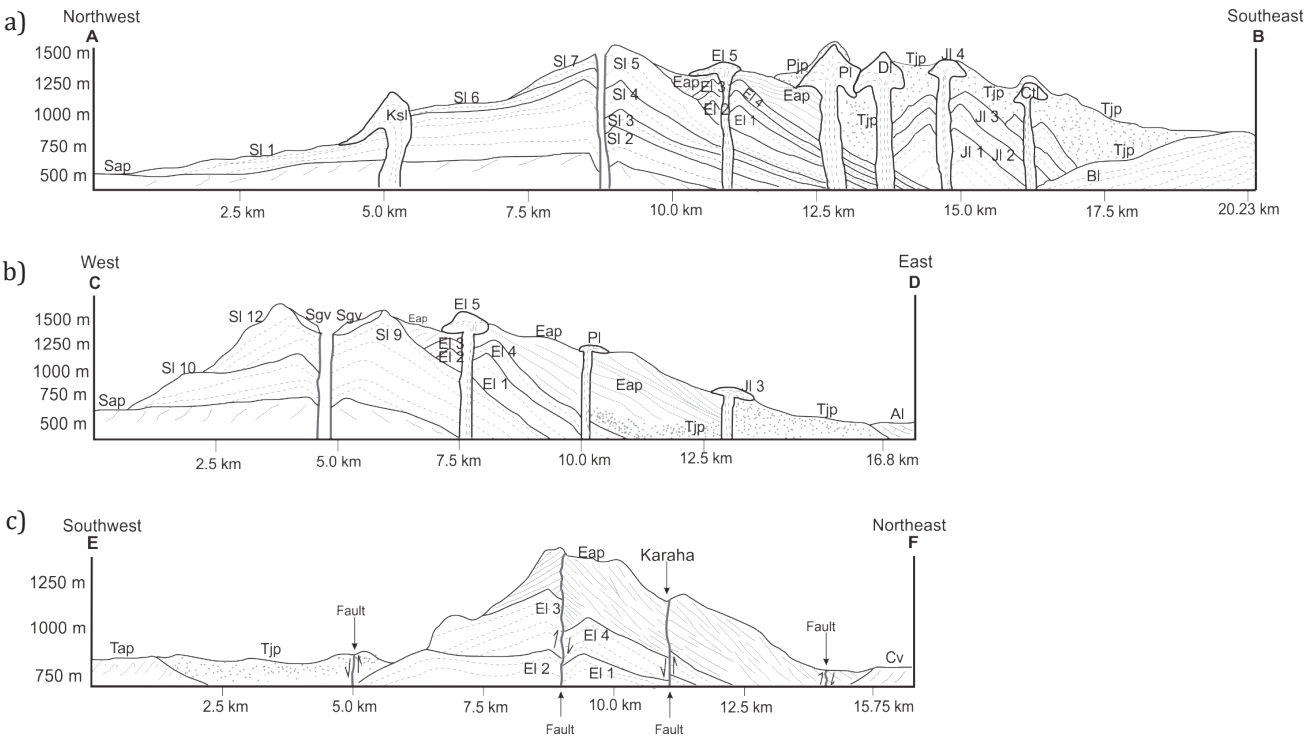

Figure 6. Three cross-sections for interpreting the subsurface structure of the Karaha-Sadakeling Volcanic Complex. a) Cross section (A-B) represents the northwestern part of study area (Sadakeling) to the Southeast (Talagabodas). b) Cross section (C-D) relatively represents the west (Sadakeling) to the east (Ewaranda and Talagabodas), and c) cross section (E-F) represents the Soutwest part of study area (Talagabodas) to Northeast part (Cakrabuana). The rock unit naming code can be seen in the stratigraphy column in Figure 5.

Within the Karaha crater complex (Figure 1b station 18; Figure 4g), pyroclastic breccia rocks have undergone strong alteration. The altered fragments and matrix have changed color to brownish white to reddish. Several points near the solfatara contain fine-grained ash deposits from phreatic eruptions (Figure 7a), 40-50 cm thick and dark brown in color (Figure 7b).

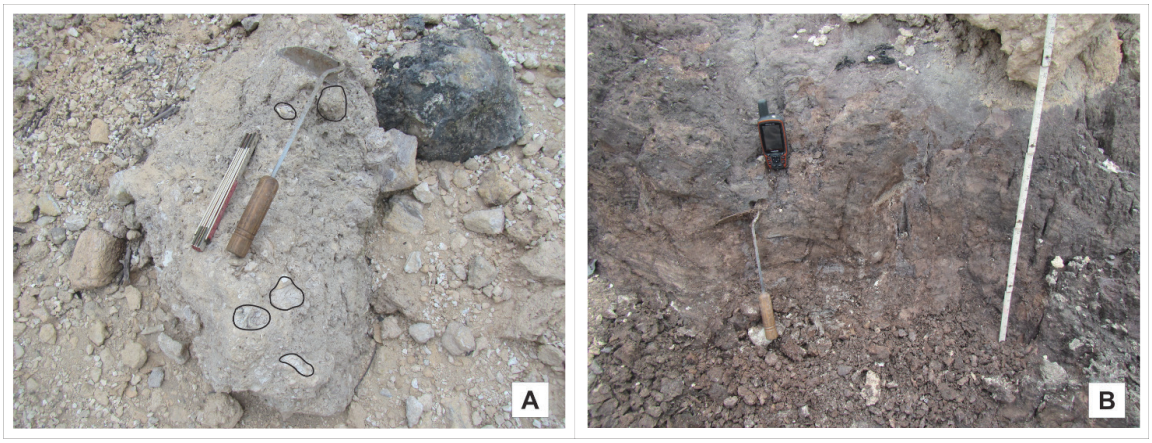

Figure 7. Strongly altered pyroclastic fragments and matrix (A), and phreatic deposits found inside Karaha Crater (B).

Talagabodas pyroclastic falls dominate and cover the southern part of the study area. The pyroclastic falls are of fine ash size, with strong weathering, basalt-composed lithics, with vesicular impressions on pumice and scoria. In this study, Talagabodas Crown, located further south than Ewaranda Crown, is only represented by approximately ¼ of the total area in the northern part of the Talagabodas Crater. Several volcanic cones that are side eruptions of Talagabodas in this study, as described in the previous subsection (Volcanic Landscape), include the Julang, Citamba, Ngantuk, Sadahurip, and Baturahong cones (see Figure 1b boundary Talagabodas Crown in the south; Figure 4 d, f, k, m). Julang volcanic cone (Jl4) (Figure 1b station 12; Figure 4f).

Rocks Properties

The lava rocks of the Karaha-Sadakeling Complex are predominantly characterized by a porphyritic texture, with plagioclase and pyroxene occurring as the dominant phenocrysts, and a groundmass composed of microlites and volcanic glass (Table 1). The lava products of the Sadakeling edifice consist mainly of basaltic andesite, represented by Sadakeling lava units Sl1, Sl5, Sl6, and Sl8 through Sl13, while basaltic compositions are identified in Sl2 and Sl3, and andesite in Sl7. Lava flows from the Ewaranda edifice are generally andesitic, except for Ewaranda lava 1 (El1), which is basaltic. In the Talagabodas edifice, lava compositions are basaltic for Baturahong lava (Bl), Ngantuk lava (Ngl), and Julang lava 1 (Jl1), whereas basaltic andesite characterizes Julang lava 2 (Jl2), Julang lava 3 (Jl3), Citamba lava (Ctl3), and Julang lava 4 (Jl4).

The specific texture of rocks that describes the dynamics of the relationship between each mineral that makes up the rock showing glomeroporphyritic, intersertal, intergranular, poikilitic, hyalopilitic, xenolith, trachyitic, and pilotassitic textures (Winter, 2001; Table 2).

Table 1. Petrography descriptions of lava of Kahara-Sadakeing Volcano Complex.

Crown	Rocks Units	Petrography			
		Mineral Assemblages	Groundmass	Texture	RockType
Ewaranda	Pl	Plag-Pyr-Olv-Opaq	Glass and Microlite	Porphyritic	Andesite
	Dl	Plag-Pyr-Olv-Opaq	Glass and Microlite	Porphyritic	Andesite
Talagabodas	Jl4	Plag-Pyr-Olv-Opaq	Microlite	Porphyritic	Basaltic andesite
	Ctl	Plag-Pyr-Opaq	Microlite	Porphyritic	Basaltic andesite
	Ngl	Plag-Pyr-Horb-Olv-Opaq	Glass and Microlite	Porphyritic	Basalt
	Jl3	Plag-Pyr-Olv-Opaq	Microlite	Porphyritic	Basaltic andesite
	Jl2	Plag-Pyr-Opaq	Microlite	Porphyritic	Basaltic andesite
	Jl1	Plag-Pyr-Olv-Opaq	Glass and Microlite	Porphyritic	Basalt
	Bl	Plag-Pyr-Olv-Opaq	Glass and Microlite	Porphyritic	Basalt

Crown	Rocks Units	Petrography			
		Mineral Assemblages	Groundmass	Texture	RockType
Ewaranda	El4	Plag-Pyr-Olv-Opaq	Microlite	Porphyritic	Andesite
	El3	Plag-Pyr-Horb-Olv-Opaq	Microlite	Porphyritic	Andesite
	El2	Plag-Pyr-Olv-Opaq	Microlite	Porphyritic	Andesite
	El1	Plag-Pyr-Olv-Opaq	Microlite	Porphyritic	Basalt
Sadakeling	Sl13	Plag-Pyr-Olv-Opaq	Glass and Microlite	Porphyritic	Basaltic andesite
	Sl12	Plag-Pyr-Olv-Opaq	Glass and Microlite	Porphyritic	Basaltic andesite
	Sl11	Plag-Pyr-Olv-Opaq	Microlite	Porphyritic	Basaltic andesite
	Sl10	Plag-Pyr-Olv-Opaq	Microlite	Porphyritic	Basaltic andesite
	Sl9	Plag-Pyr-Olv-Opaq	Glass and Microlite	Porphyritic	Basaltic andesite
	Sl8	Plag-Pyr-Olv-Opaq	Microlite	Porphyritic	Basaltic andesite
	Sl7	Plag-Pyr-Olv-Opaq	Microlite	Porphyritic	Andesite
	Sl6	Plag-Pyr-Olv-Opaq	Microlite	Porphyritic	Basaltic andesite
	Sl5	Plag-Pyr-Olv-Opaq	Glass and Microlite	Porphyritic	Basaltic andesite
	Sl4	Plag-Pyr-Olv-Opaq	Microlite	Porphyritic	Andesite
	Sl3	Plag-Pyr-Olv-Opaq	Glass and Microlite	Porphyritic	Basalt
	Sl2	Plag-Pyr-Olv-Opaq	Glass and Microlite	Porphyritic	Basalt
	Sl1	Plag-Pyr-Olv-Opaq	Microlite	Porphyritic	Basaltic andesite

Note: Plag; Plagioclase, Pyr:Pyroxene, Olv: Olivine

Table 2. The specific texture of the relationship between minerals in lava rocks at the Karaha-Sadakeling Volcanic Complex.

Crown	Rocks Unit	Rocks Textures								
		Intrg	Intrs	Glmrp	Plts	Pltc	Vtrp	Hypl	Trac	Xen
Ewaranda	Pl	v	v	v	*			*	v	
	Dl	*	v	v		v		v		
Talagabodas	Jl4	v	v	v				v		
	Ctl	v	*	*	*	v			v	
	Ngl		v	v	v				v	
	Jl3	*	v	v					v	v
	Jl2		v	v		v		v		
	Jl1	v	v	*						v
	Bl	*	*	v		v				
Ewaranda	El4			v			v			v
	El3	*	v	*					v	
	El2	*		v			v			
	El1	v	v	v		v				
Sadakeling	Sl13	*	*	*		v		v		v
	Sl12	v	v	v		v				
	Sl11	v	v	*				v		v
	Sl10		v	v				v		v
	Sl9	*	*	v		v		v		v
	Sl8	*	*	v		v		v		v
	Sl7		*	v	v	v	*	v		
	Sl6	v	*	v	v	v				
	Sl5	*	*	v		v	v	v		
	Sl4	*	v	v		v			v	
	Sl3	*	v	v					v	
	Sl2	*	*	v		v				
	Sl1	*	*	v		v			v	v

Note: Intrg: Intergranular, Intrs: Intersertal, Glmrp: Glomeroporphyritic, Plts: Pilotassitic, Pltc: Poikilitic, Vtrp: Vitrophyric, Hypl: Hyalopilitic, Trac: Trachytic, Xen: Xenolith. Code v; dominant, *; present but not dominant.

Table 3. Microtexture of plagioclase of lava rocks at the Karaha-Sadakeling Volcanic Complex.

Crown	Rocks Units	Microtexture Plagioclase									
		FSOZ	RZC	CS	FS	RS	S	St	Gc	Mc	BC
Ewaranda	Pl	v	v	v	v	*	v		v	v	v
	Dl	v	v	v	v	v	v		v	v	v
Talagabodas	Jl4	v	v	v	v	v	v	v	v	v	v
	Ctl	v	v	v	*	v	v	v	*	v	v
	Ngl	*	v	v	v	v	v		v	v	v
	Jl3	v	v	v	v	*	v		v	v	v
	Jl2	v	v	v	v	v	v		v	v	v
	Jl1	v	v	v	v	v	v	*	v	v	v
	Bl	v	v	v	v	v	v	*	*	v	v
Ewaranda	El4	v	v	*	v	v	v	v	*	v	v
	El3	v	v	v	v	*	*	*	v	v	v
	El2	v	v	v	v	v	v	*	v	v	v
	El1	v	v	v	v	v	v	*	v	v	v
Sadakeling	Sl13	v	v	v	v	v	v		*	v	v
	Sl12	v	v	v	*	v	v			v	v
	Sl11	v	v	v	v	v	v	*	*	v	v
	Sl10	v	*	v	v	v	v		v	v	v
	Sl9	v	v	v	v	v	v			v	v
	Sl8	v	v	v	v	v	v	*	v	v	v
	Sl7	v	v	v	v	*	*		v	v	v
	Sl6	v	v	v	v	v	v		*	v	v
	Sl5	v	v	v	v	v	v	*	v	v	v
	Sl4	v	v	v	v	v	v	*	v	v	v
	Sl3	v	v	v	v	v	v		v	v	v
	Sl2	v	v	v	v	v	v	*	v	v	v
	Sl1	v	v	v	v	v	v		v	v	v

Note: FSOZ: Fine Scale Oscillatory Zoning, RZC: Rounded Zone Corner, CS: Coarse Sieve, FS: Fine Sieve, RS: Resorption Surface, S: Synneusis, St: Swallow-tail, Gc: Glomerocrysts, Mc: Microlites, BC: Broken Crystal. Symbol v refers to dominant, and * present but not dominant.

Table 3 presents microtexture data of plagioclase minerals from each lava rock unit in the Karaha-Sadakeling Volcanic Complex (Renjith, 2014). Broken crystals and microlites are dominant in each lava rock, followed by sieve, zoning, synneusis, glomerocrysts, and swallow-tail textures. Broken crystal is defined as an open crack or fissure that cuts the main crystal body into separate fragments and is formed due to the accumulation of stress during fragmentation caused by the rate of decompression (Miwa and Geshi, 2012).

5. Discussions

Volcanostratigraphy

The volcanic evolution of the Karaha-Sadakeling Complex initiated with the activity of Mount Cakrabuana in the northeastern sector of the study area, followed by the development of the Sadakeling, Talagabodas volcanic cones toward the south, and Ewaranda, located in the central part of the study area. The stratigraphic succession of eruption products reveals significant overlaps among the deposits of each volcanic center, which are clearly exposed across the northern, central, and southern parts of the complex.

Some of the rock outcrops found in the field are covered by pyroclastic fall deposits from the younger Crown (Talagabodas Crown), especially in the southern part of Ewaranda. The eruption of Sadakeling is generally characterized by a central eruption that includes lava flows, pyroclastic flows, and the formation of the Kersamanah cone in the north which is the result of the side eruption of Sadakeling Crown.

Sadakeling and Ewaranda are interpreted to have originated as a single volcanic edifice that subsequently underwent a shift in its eruptive center. This interpretation is supported by the presence of a lava flow ridge in the northeastern sector of Sadakeling, which indicates that the flow was sourced from the flanks of the Ewaranda Crater, later modified by a sector collapse. Additional evidence is provided by the Sadakeling 9 lava unit (Sl 9), which forms a prominent ridge separating the Sadakeling Crater to the west from the Ewaranda Crater to the east (see Sl 2, Sl 3, Sl 4, Sl 5, and Sl 9 on the volcanostratigraphic map Figure 5, and cross-sections A–B and C–D in Figure 6).

Following the Sadakeling and Ewaranda phases, volcanic activity migrated southward, producing a sequence of deposits ranging from lava flows to pyroclastic flows and pyroclastic fall deposits of Talagabodas, with fall deposits dominating the southern sector of the study area. In the central part of the complex, Ewaranda Crown is characterized by a distinctive morphology of southward crater wall collapse, likely associated with explosive eruptions that generated extensive pyroclastic flow deposits (Eap). Several minor volcanic cones in the southern area, including Kidang, Putri, and Dirgahayu, are interpreted as products of side eruptions of Ewaranda Crown. Putri pyroclastic fall (PJp) is the youngest eruption product of Ewaranda Crown, and most likely occurred after the deposition of pyroclastic fall products of Talagabodas (Tjp) in the southern part of the study area, and after deposition of Ewaranda pyroclastic flow (Eap). This is based on the textural appearance of the outcrops found in the field (see Figure 4 m and k for Talagabodas pyroclastic fall (Tjp), and 4n for Putri pyroclastic fall (PJp)). This phase indicates that following the Talagabodas activity in the south, volcanic activity subsequently re-focused at Ewaranda in the central part of the study area (Figure 5).

In the southern sector, volcanic cones associated with Talagabodas Crown namely Sadahurip, Ngantuk, Julang, and Citamba are predominantly covered by thick pyroclastic fall deposits (see code k and m in Figures 4 and 5). As noted by Asmoro (2013), the Sadahurip cone represents a flank eruption of Talagabodas, consisting of alternating lava flows and subsequently overlain by pyroclastic fall deposits from Talagabodas dated to approximately 13,320 BP.

The distribution pattern of volcanic cones has a similar pattern with the estimated main structure which is relatively northwest-southeast oriented. The regional geologic map of Tasikmalaya Sheet by Budithrisna (1996) with a scale of 1:100 000 shows that there is one main fault that is regionally from Malangbong in the north to the southeast and cuts young volcanic rocks and old volcanic rocks. Then in the Karaha-Sadakeling complex there are local faults that are in the relatively same direction, northwest-southeast (Figures 1b and c, 5, and 6c).

Analysis of the distribution pattern of volcanic cones and volcanic craters in the study area shows a similar pattern to the main fault structure pattern of the study area. Volcanic cones and crater traces from the northern part of the study area to the south show a northwest-southeast distribution direction (Figures 1b, 5, and 6c). According to Danakusumah and Suryantini (2020), geological structures identified through alignment patterns in the Karaha geothermal complex are generally northwest-southeast and northwest-southwest oriented and are active faults and become the main permeable pathway for fluids. This condition indicates the relationship between volcanic activity and the geological structure of the study area. According to Cembrano and Lara (2009), the association of volcanism can be directly related to active geological structures or passively reactive old faults, which can then affect volcanic activity. In addition, geothermal areas can be hot fluid pathways that influence fluid characteristics (Andrianaivo and Ramasiarinoro, 2010)

Crystal Fractionation and Magma Dynamic

The petrogenetic framework of the study area is characterized through petrographic analyses of mineral composition, textural relationships among lava rock minerals, and plagioclase microtextures (Tables 1-3). The compositional evolution of magma from Sadakeling–Talagabodas–Ewaranda indicates a transition from basaltic andesite and subsequently to andesite. Plagioclase and pyroxene commonly occur as phenocrysts, whereas the groundmass is predominantly composed of plagioclase microlites and volcanic glass (Table 1; Figure 8). The rock texture that shows the relationship between each mineral in the rock indicates that crystal fractionation is the most dominant process which is found in every lava sample from each Crown (Table 2). This texture is characterized by the appearance of plagioclase and pyroxene phenocrystals clustered into aggregates or glomeroporphyritic (Figure 8I). The fusion of phenocryst between plagioclase and pyroxene occurs due to synneusis, crystal accumulation occurs due to surface tension and bonding through intercrystalline penetration due to crystal growth that has a lower density than the surrounding magma density (Cox et al., 1979; Deer et al., 2013; Vernon, 2008).

The cooling process and thermal gradients, reflected in variations in mineral nucleation and groundmass crystallization rates, are expressed by the occurrence of intergranular and intersertal textures (Figure 8a–b). Intersertal texture is defined by volcanic glass occupying the spaces between phenocrysts, whereas intergranular texture is characterized by smaller crystals infilling the interstices between two or more phenocrysts (Cox et al., 1979; Winter, 2001). A poikilitic texture forms as a result of the variation in nucleation and growth rates among minerals, whereby single crystals nucleate and grow to relatively large sizes under low nucleation rates, whereas other minerals with higher nucleation rates remain small and gradually become enclosed within the larger crystals (Vernon, 2008; Cox et al., 1979; Winter, 2001). The poikilitic texture, illustrated in Figure 8c by pyroxene crystals growing randomly within plagioclase, is predominantly observed in the Sadakeling Phase (Table 2).

The pilotassitic texture reflects dynamic processes within the magma, resulting from differential motion, and is characterized by the presence of subparallel microclasts (Cox et al., 1979; Deer et al., 2013; Vernon, 2008). The pilotassitic texture, illustrated in Figure 8d, is observed in Sl 6, Sl 7, Ctl, Ngl, and Pl. When nucleation and subsequent crystal growth are absent, phenocrysts embedded within a glassy matrix define a vitrophyric texture (Vernon, 2008; Cox et al., 1979; Winter, 2001). The vitrophyric texture is exclusively observed in Sl 5, Sl 7, El 2, and El 4 (Figure 8e and f). The hyalopilitic texture is characterized by a groundmass composed of small, parallel-aligned feldspar microlites embedded within volcanic glass (Cox et al., 1979; Deer et al., 2013; Vernon, 2008; Winter, 2001). The hyalopilitic texture is identified in Sl 5, Sl 7–Sl 11, and Sl 13 (Figure 8g). The trachytic texture is characterized by the alignment of microlites into flow lines around phenocrysts, resulting from viscous magma flow during effusive eruptions and the differential movement of microlites (Vernon, 2008). The trachytic texture is observed in Sl 1, Sl 3, Sl 4, El 3, Pl, Jl 3, Ngl, and Ctl (Figure 8J). The xenolith texture is defined by the incorporation of older rock fragments within the magma (Cox et al., 1979; Deer et al., 2013; Vernon, 2008). The xenolith texture is identified in Sl 1, Sl 8–Sl 11, Sl 13, El 4, Jl 1, and Jl 3 (Figure 8h).

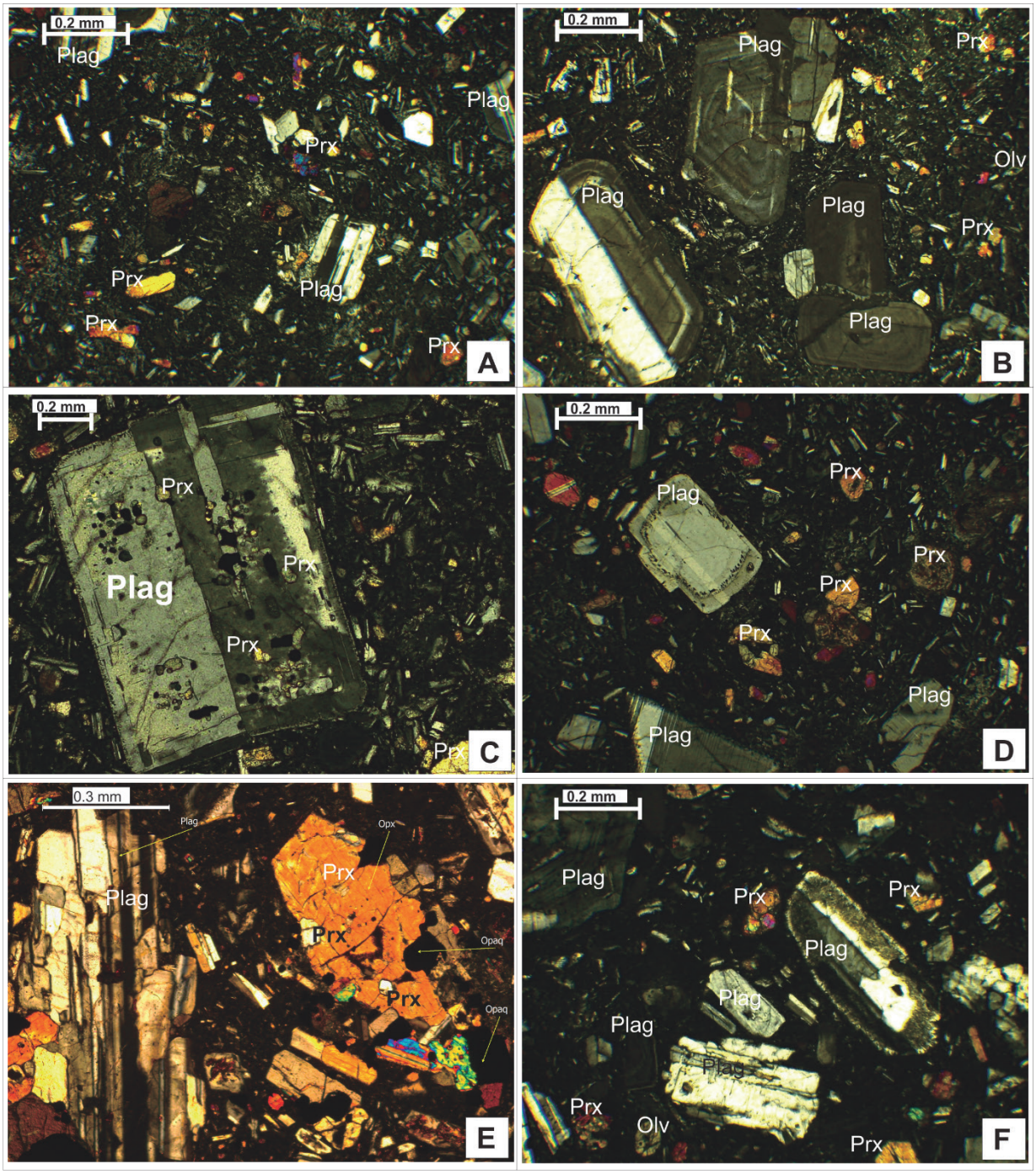

Figure 8. Photomicrographs illustrating specific rock textures within the Karaha-Sadakeling Volcanic Complex are presented. (a) Depicts the intersertal texture, which creates the impression that the spaces between the Plagioclase (Plag) and Pyroxene (Prx) crystals are predominantly filled with volcanic glass. (b) Represents the intergranular texture, where the voids between the phenocrysts of Plagioclase and Pyroxene are occupied by smaller mineral grains. (c) Illustrates the poikilitic texture, marked by the presence of pyroxene minerals that grow irregularly within the Plagioclase matrix. (d) Showcases the pilotassitic texture, characterized by plagioclase microlites arranged around phenocrysts in a subparallel orientation. The vitrophyric texture is represented in parts (e) and (f); part (e) features plagioclase and pyroxene phenocrysts embedded in a volcanic glass groundmass, while part (f) displays predominant plagioclase phenocrysts within a volcanic glass matrix. Part (g) presents a hyalopilitic texture, characterized by microlite minerals set within a volcanic glass groundmass. (h) Illustrates a xenolith texture, defined by foreign rock fragments adjacent to pyroxene and olivine minerals. The glomerporphyritic texture is depicted in (i), characterized by aggregates of plagioclase and pyroxene minerals that are fused, and (j) Features a trachytic texture characterized by a flow pattern of plagioclase microlites surrounding plagioclase phenocrysts.

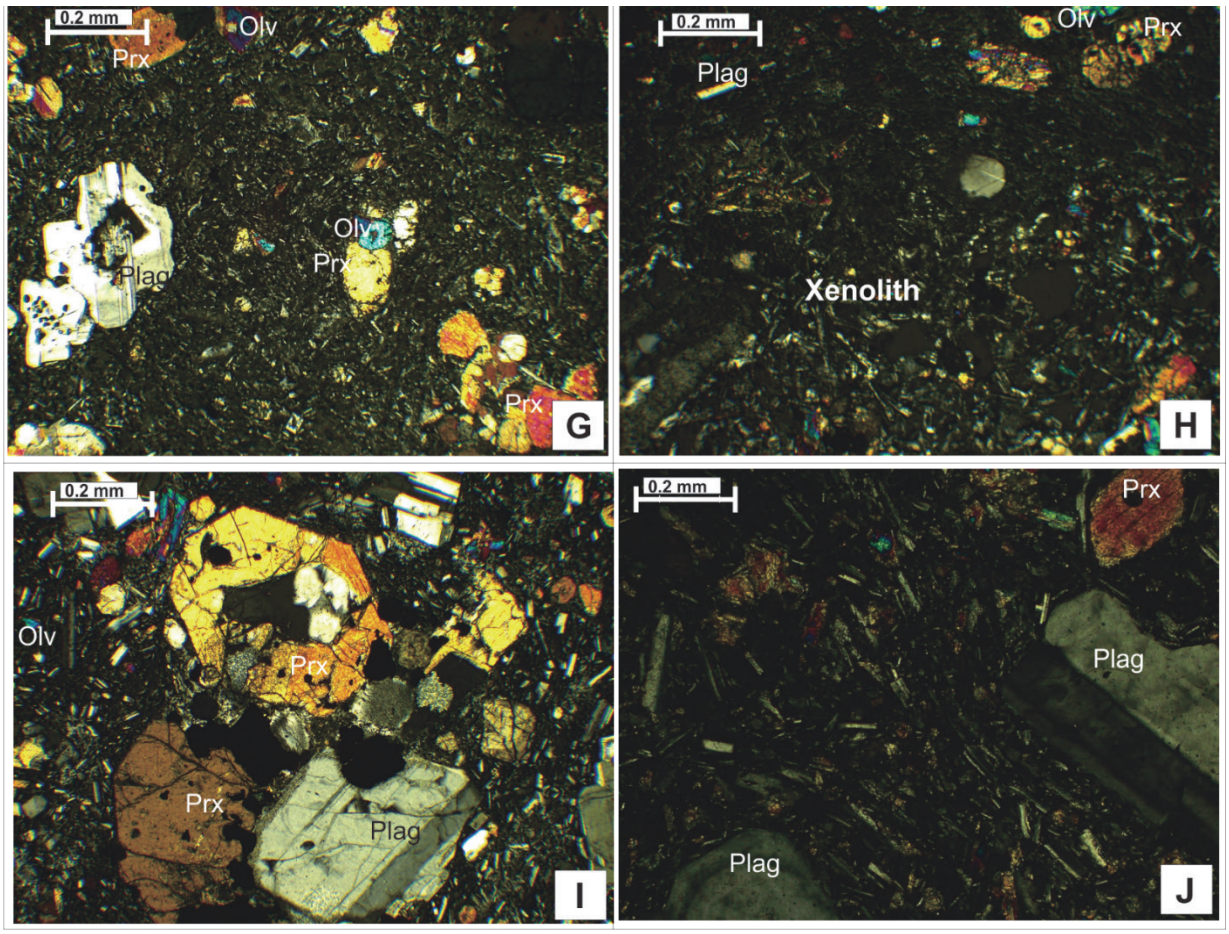

Figure 8 (continued).

Plagioclase microtextures commonly coexist within individual plagioclase crystals (Table 3; Figure 9). This coexistence reflects dynamic magmatic processes operating within the magma chamber, persisting up to the time of eruption.

The presence of broken crystal (BC) texture is indicative of a rapid decompression rate during eruption, stemming from the release of gas trapped under high pressure. This texture is characterized by euhedral crystals exhibiting irregularly fractured edges, with no indications of subsequent regrowth (Best and Christiansen, 1997; Miwa and Geshi, 2012; Renjith, 2014; Figure 9i and j). Conversely, the microlite (Mc) texture in plagioclase, which constitutes the primary mass, arises from an increased degree of syneruptic cooling (Blundy and Cashman, 2005; Toramaru et al., 2008; Figure 9f). If the cooling rate continues to increase, the microlite plagioclase crystals at the time of eruption will form a swallowtail texture (St) (Figure 9h). This condition occurred due to rapid growth caused by excessive cooling associated with the eruption (Renjith, 2014; Viccaro et al., 2012).

Sieve texture groups are generally formed under pre-eruption conditions that describe growth processes in the magma chamber due to changes in temperature, H_2O content, pressure, decompression rate, and magma composition (Renjith, 2014). The coarse sieve (CS) texture is formed as a result of the dissolution process of An-rich magma from deeper magma chambers rising to shallower magma chambers undergoing dissolution, and the quality apparent in the texture indicates the intensity of the dissolution process controlled by differences in the rate of decompression and H_2O content (Renjith, 2014; Viccaro et al., 2010; Figure 9a, d, g, and j). Meanwhile, the fine sieve (FS) texture indicates crystallization of less differentiated magma, representing a period of dissolution due to interaction with more primitive magma (Renjith, 2014; Tsuchiyama, 1985; Figure 9d and j).

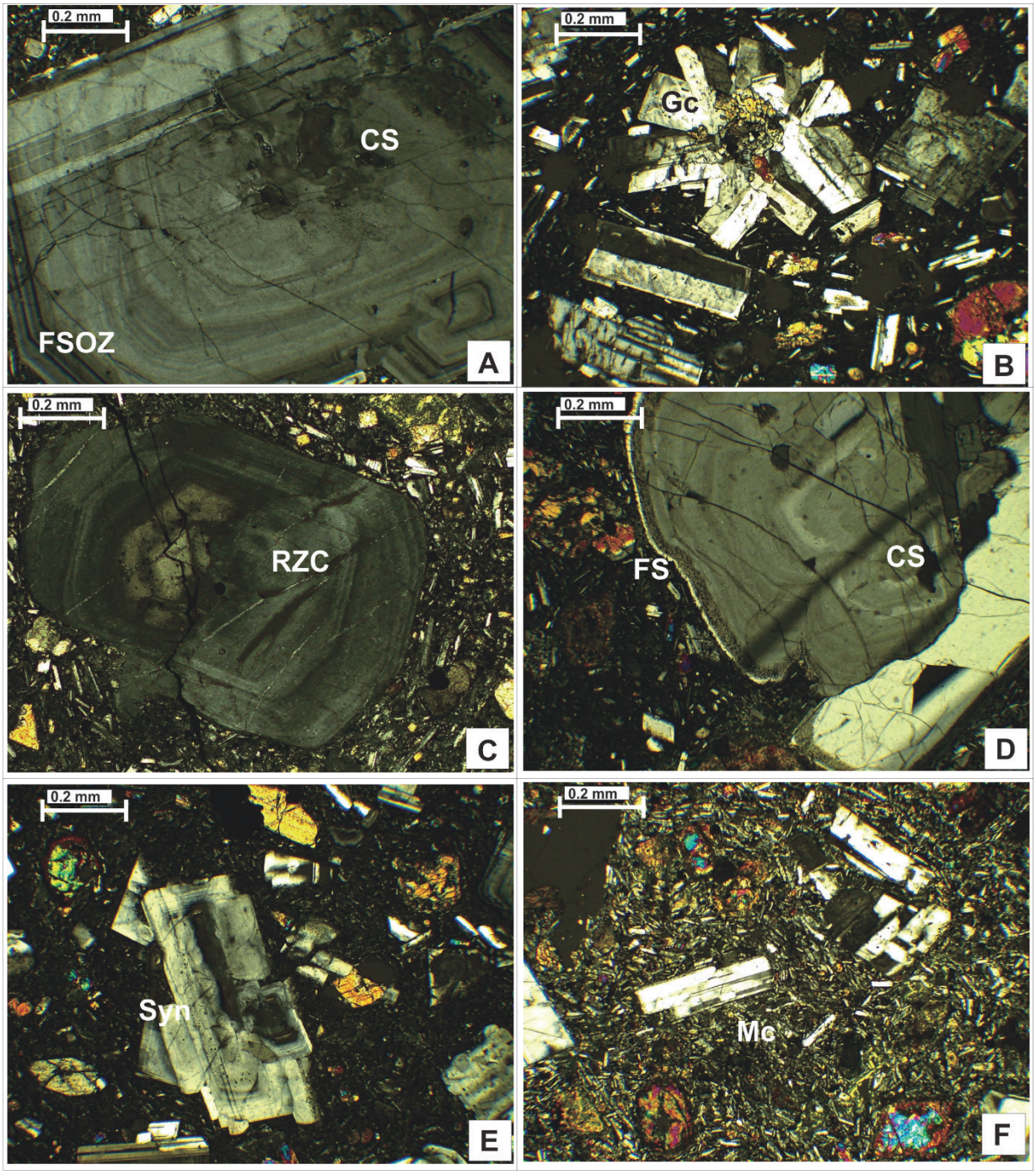

Figure 9. Multiple micro-textures of Plagioclase. (a) Fine-scale oscillatory zoning and coarse sieve textures; (b) glomerocryst texture; (c) rounded zone corner texture; (d) fine sieve and coarse sieve textures; (e) synneusis texture; (f) microlite texture; (g) resorption surface and coarse sieve textures; (h) resorption surface, fine scale oscillatory zoning, and swallow tail textures, (i) broken crystal texture; and (j) fine Sieve, coarse sieve, broken crystal, rounded zone corner and resorption surface textures. Abbreviations: FSOZ = Fine-scale oscillatory zoning; CS = Coarse sieve; Gc = Glomerocryst; RZC = Rounded zone corner; FS = Fine sieve; Syn = Synneusis; Mc = Microlite; BC = Broken crystal; RS = Resorption surface; St = Swallow-tail.

The glomerocryst texture is defined by the aggregation of two or more plagioclase crystals that have fused to form composite clusters (Renjith, 2014; Figure 9b). In the analyzed samples, these aggregated plagioclase crystals display well-developed zoning, suggesting that dissolution processes occurred before the fusion event. This observation implies that crystal resorption preceded aggregation, reflecting dynamic magmatic conditions during crystallization and subsequent crystal interaction within the magma chamber.

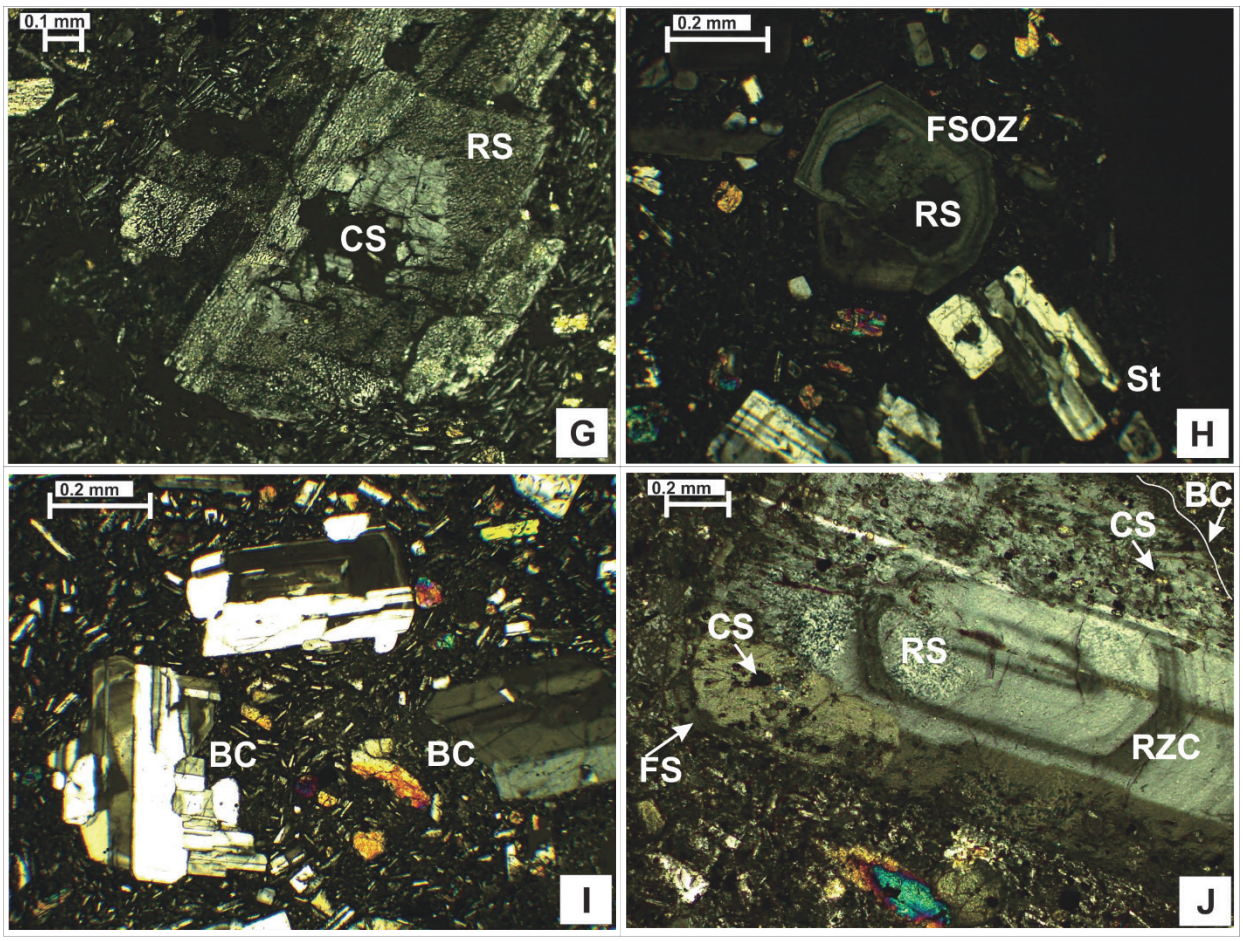

Figure 9 (continued).

The zoning textures of lavas in the study area are predominantly developed along the rims of plagioclase crystals, with some extending inward toward the crystal cores. Fine-scale oscillatory zoning (FSOZ) is observed in several samples, manifested as curved to slightly wavy patterns along crystal margins and defined by subtle color variations within the zoning (Figure 9a and h). Such features are indicative of concurrent dissolution and magmatic reactions during crystal growth (Vance, 1962; Pearce and Kolisnik, 1990). In addition, rounded zone corner (RZC) textures are observed under the microscope, characterized by oval to circular domains near the cores of plagioclase crystals (Figure 9c and j). These textures are interpreted to result from minor dissolution as crystals traversed magmatic gradients (Renjith, 2014).

Resorption surface (RS) textures are distinguished by irregular crystal boundaries, typically expressed as unevenly distributed white and black patches or grains (Figures 9g and j). These features are interpreted as the result of intense and prolonged dissolution during interactions with more primitive magma (Renjith, 2014). The development of major resorption zones is attributed to the injection of less evolved magma, which promotes rapid magma ascent and plagioclase mobilization. This process enhances magma mixing while simultaneously inducing rapid, kinetically controlled crystal growth (Pietranik et al., 2006).

The synneusis (Syn) texture is characterized by the adhesion of plagioclase crystals, reflecting dynamic interactions within a convecting magma chamber (Renjith, 2014; Figure 9e). According to Gogoi and Saikia (2018) and Vance (1969), this texture is formed by the process of magma assimilation and is controlled by segregation between crystals, orientation, and the morphological boundaries of adjacent crystals.

Volcanic Hazard Map

Field observations combined with volcanostratigraphic relationships indicate that present-day volcanic activity is concentrated within the Karaha Crater Complex, which represents the youngest volcanic center (Ewaranda Crown) in the study area. Current manifestations include solfatara fields, hot springs, mud pools, fumaroles, and associated alteration of pyroclastic rocks and phreatic deposits (Figure 7). These features suggest that the primary volcanic hazard potential in the region is most likely to originate from the Karaha Crater. Chronological comparisons provide additional context. Chalcedony formation dated by conventional radiocarbon methods from lake sediments in Mount Candramerta, located south of Mount Sadahurip, yielded an age of 5910 ± 76 years BP (Moore et al., 2002). Historical records further indicate a phreatic eruption at Mount Putri in May 1861 (Global Volcanism Program Gunung Putri, 2013). Consistent with these findings, geothermal manifestations are typically associated with the flanks of andesitic volcanoes (Corbett and Leach, 1998), and the Karaha Complex geothermal reservoir is known to be dominated by pyroclastic deposits (Moore et al., 2008).

Based on the analysis of these parameters and considering the topographic cross-section (Figure 6b and c), we propose that if Karaha Crater experiences increased volcanic activity, the types of hazards that may occur include pyroclastic falls, pyroclastic flows, and lava flows, with the direction of lava and pyroclastic flows towards the east-northeast sector of Karaha (Figure 10).

For pyroclastic hazards, within a radius of 3-5 km, which is the outer ring (yellow circle), there is the potential for ashfall and a small amount of incandescent rock ejection, as well as the expansion of lava and pyroclastic flows. Within a radius of 1-3 km (pink circle), there is the potential for heavy ashfall and incandescent rock ejections, as well as lava flows and pyroclastic flows. Within a radius of 0-1 km (red circle), there is a high potential for heavy pyroclastic fallout, lava flows, and pyroclastic flows.

6. Conclusions

This study investigates volcanic landforms, rock observations and sampling, stratigraphic analysis, and volcanic hazard potential within the Karaha-Sadakeling Volcanic Complex. The volcanic evolution of the area progressed sequentially, beginning with the formation of Cakrabuana in the northeastern sector, followed by the development of Sadakeling, Ewaranda, and Talagabodas, before volcanic activity shifted back to the Ewaranda complex. This later stage was characterized by the deposition of pyroclastic fall products from Mount Putri and the formation of the Karaha Crater. Geological evidence suggests that Sadakeling and Ewaranda initially constituted a single volcanic edifice that underwent a shift in its eruptive center, culminating in the collapse of Ewaranda and the generation of extensive pyroclastic deposits.

The volcanic landscape of the study area reflects a sequential evolution of eruptive products: Cakrabuana in the northeast, Sadakeling in the northwest dominated by lava flows, Ewaranda in the central sector characterized by pyroclastic flow deposits, and Talagabodas in the south represented by extensive pyroclastic fall deposits. The dominant lava types record a compositional progression from basaltic andesite (Sadakeling and Talagabodas) to andesite (Ewaranda). Petrogenetic analysis of the lava rocks indicates complex magmatic processes operating from the deep to shallow magma chamber, as well as dynamic conditions during eruption. These processes include crystal fractionation, decompression associated with the injection of primitive magma, magma mixing driven by convective currents, thermal overprinting from replenishment by primitive magma, cooling related to eruptive events, and decompression linked to eruptive activity.

Based on field observations and their relationship with volcanostratigraphy, as an effort for future mitigation, an analysis of potential hazards in the form of volcanic hazards originating from Karaha Crater was conducted, with the types of hazards being pyroclastic fall, pyroclastic flow, lava flow, and lahar flow.

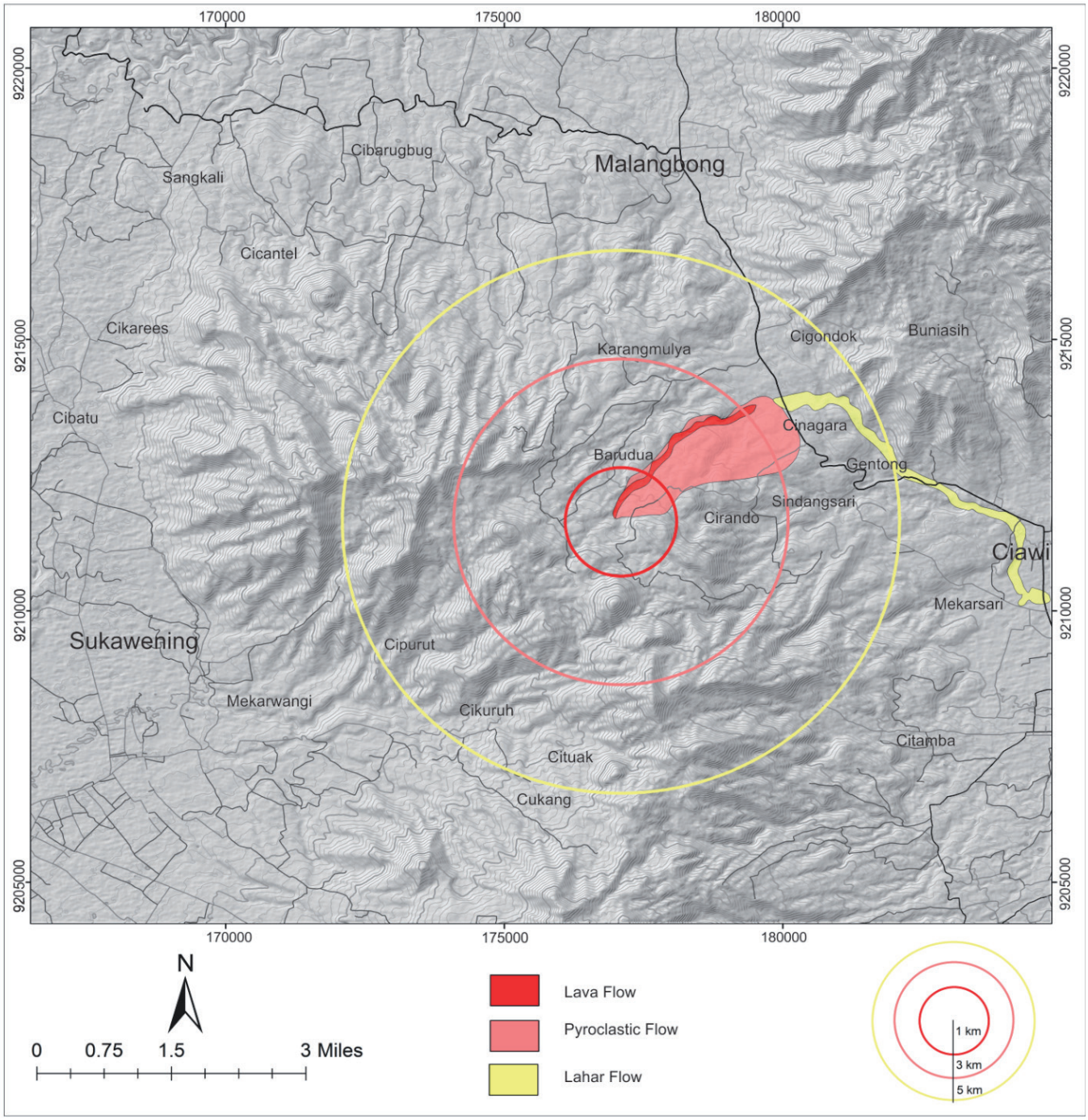

Figure 10. Volcanic hazard and zonation map of Karaha Crater derived from field observations and volcanostratigraphy analysis.

Acknowledgments

We would like to thank the Center for Volcanology and Geological Hazard Mitigation (CVGHM), Geological Agency, for providing the first author with the opportunity and funding to collect samples in 2021, as well as the Galunggung volcano observers who accompanied us in the field. We would also like to express our gratitude to CVGHM for permission to use a microscope during petrography analysis. We thank the reviewers for their suggestions and recommendations for the improvement of this paper.

References

Abdurrachman, M., 2012. Geochemical variation of Quaternary volcanic rocks in Papandayan area, West Java, Indonesia: A role of crustal component. 12th Reg. Congr. Geol. Miner. Energy Resour. Southeast Asia (GEOSEA 2010), Bangkok, Thailand, Spec. Issue.

Alzwar, M., Akbar, N., Bachri, S., 1992. Peta Geologi Lembar Garut dan Pameungpeuk, Jawa, skala 1:100.000. Puslitbang Geologi, Bandung.

Andrianaivo, L., Ramasiarinoro, V.J., 2010. Relation between regional lineament systems and geological structures: Implications for understanding structural controls of geothermal system in the volcanic area of Itasy, Madagascar. Proc. World Geotherm. Congr.

Arisbaya, I., Aldinofrizal, A., Sudrajat, Y., Gaffar, E.Z., Harja, A., 2018. Model sistem panas bumi lapangan Karaha-Talaga Bodas berdasarkan inversi 2D data megnetotellurik. Riset Geol. Pertamb. 28, 221–234.

Asmoro, P., 2013. Geology of Mount Sadahurip, Garut, District. [Nama Jurnal Tidak Lengkap] 14, 1–10.

Badan Informasi Geospasial, 2018. Ina-Geoportal. https://tanahair.indonesia.go.id/portal-web/.

Best, M.G., Christiansen, E.H., 1997. Origin of broken phenocrysts in ash-flow tuffs. GSA Bull. 109, 63–73.

Blundy, J., Cashman, K., 2005. Rapid decompression-driven crystallization recorded by melt inclusions from Mount St. Helens volcano. Geology 33, 793–796.

Bronto, S., 1989. Volcanic geology of Galunggung, West Java, Indonesia. [Disertasi/Tesis]. University of Canterbury.

Bronto, S., Koswara, A., 2006. Stratigrafi gunung api daerah Bandung Selatan, Jawa Barat. J. Geol. Indones. 1, 89–101.

Bronto, S., Sianipar, J.Y., Pratopo, A.K., 2016. Volcanostratigraphy for supporting geothermal exploration. IOP Conf. Ser.: Earth Environ. Sci. 42, 012014.

Budhitrisna, T., 1986. Geologic map of the Tasikmalaya Quadrangle, West Java. Directorate Geology, Ministry of Energy and Mineral Resources.

Cembrano, J., Lara, L., 2009. The link between volcanism and tectonics in the southern volcanic zone of the Chilean Andes: A review. Tectonophysics 471, 96–113.

Corbett, G.J., Leach, T.M., 1998. Southwest Pacific Rim Gold-Copper Systems: Structure, Alteration, and Mineralization. Society of Economic Geologists, Spec. Publ. 6.

Cox, K.G., Bell, J.D., Pankhurst, R.J., 1979. The Interpretation of Igneous Rocks. Springer, Netherlands.

Danakusumah, G., Suryantini., 2020. Integration of the lineament study in the Karaha-Bodas geothermal field, West Java. IOP Conf. Ser.: Earth Environ. Sci. 417, 012008.

Deer, W.A., Howie, R.A., Zussman, J., 2013. An Introduction to the Rock-Forming Minerals, third ed. The Mineralogical Society, London.

Global Volcanism Program, 2013. Gunung Putri. Smithsonian Institution. https://volcano.si.edu/volcano.cfm?vn=263160.

Gogoi, B., Saikia, A., 2018. Synneusis: Does its preservation imply magma mixing? Mineralogia 49, 99–117.

Groppelli, G., Molist, J.M., 2013. Volcanic stratigraphy—State of the art. Ciênc. Terra 18, 1–15.

Haryanto, I., 2006. Sruktur geologi paleogen dan neogen di Jawa Barat. Kumpulan Buletin Geologi 4, 1–12.

Haryanto, I., 2013. Struktur sesar di Pulau Jawa bagian barat berdasarkan hasil interpretasi geologi. Bull. Sci. Contrib. 11, 10–20.

Haryanto, I., Setiadi, D.J., Alam, S., Ilmi, N.N., Sunardi, E., 2018. Mountain-front sinuosity and asymmetrical factor of Leles-Garut intra-arc basin, West Java. J. Geol. Sci. Appl. Geol. 2, 5.

Irada, A., 2017. Interaksi fluida dan batuan berdasarkan mineral ubahan di sumur KRH 5-2 lapangan panas bumi Karaha Bodas provinsi Jawa Barat. M.Sc. Thesis, Institut Teknologi Bandung.

Katili, J.A., 1975. Volcanism and plate tectonics in the Indonesian island arcs. Tectonophysics 26, 165–188.

Katili, J.A., Sudradjat, A., 1984. Galunggung, the 1982–1983 Eruption: Volcanological Survey of Indonesia. Directorate General of Geology and Mineral Resources, Bandung.

Kausar, A.A., Indarto, S., Yuliyanti, A., 2016. Petrologi dan geokimia batuan vulkanik kompleks panasbumi Talagabodas-Karaha Garut, Jawa Barat. J. Geol. Sumberdaya Miner. 17, 1–14.

Kausar, A.A., Setiawan, I., Yuliyanti, A., Lintjewas, L., Jakah, J., Herawan, W., 2024. Geochemical characteristics of volcanic rocks in the Karaha – Talagabodas fields related to Galunggung Volcano. Riset Geol. Pertamb. 34, 25–40.

Keskin, M., Pearce, J.A., Mitchell, J.G., 1998. Volcano-stratigraphy and geochemistry of collision-related volcanism on the Erzurum–Kars Plateau, northeastern Turkey. J. Volcanol. Geotherm. Res. 85, 355–404.

Lockwood, J.P., Hazlett, R.W., 2013. Volcanoes: Global Perspectives. John Wiley & Sons, Chichester.

Martodjojo, S., Djuhaeni., 1996. Sandi Stratigrafi Indonesia. IAGI, Jakarta.

Miwa, T., Geshi, N., 2012. Decompression rate of magma at fragmentation: Inference from broken crystals in pumice of vulcanian eruption. J. Volcanol. Geotherm. Res. 227–228, 76–84.

Moore, J.N., Allis, R.G., Nemcok, M., Powell, T.S., Bruton, C.J., Wannamaker, P.E., Raharjo, I.B., Norman, D.I., 2008. The evolution of volcano-hosted geothermal systems based on deep wells from Karaha-Telaga Bodas, Indonesia. Am. J. Sci. 308, 1–48.

Moore, J.N., Allis, R., Renner, J.L., Mildenhall, D., McCulloch, J., 2002. Petrologic evidence for boiling to dryness in the Karaha-Telaga Bodas geothermal system, Indonesia. Proc. 27th Workshop Geotherm. Reserv. Eng., Stanford.

Muhammad, A.E.P., Abdurrachman, M., Nugraha Kartadinata, M., Banggur, W.F., 2025. Petrogenesis of Sadakeling – Karaha Volcanic Complex, Tasikmalaya, West Java, Indonesia: Argoland contamination. IOP Conf. Ser.: Earth Environ. Sci. 1451, 012021.

Pearce, T.H., Kolisnik, A.M., 1990. Observations of plagioclase zoning using interference imaging. Earth-Sci. Rev. 29, 9–26.

Petterson, M.G., Treloar, P.J., 2004. Volcanostratigraphy of arc volcanic sequences in the Kohistan arc, North Pakistan: Volcanism within island arc, back-arc-basin, and intracontinental tectonic settings. J. Volcanol. Geotherm. Res. 130, 147–178.

Pietranik, A., Koepke, J., Puziewicz, J., 2006. Crystallization and resorption in plutonic plagioclase: Implications on the evolution of granodiorite magma (Gęsiniec granodiorite, Strzelin Crystalline Massif, SW Poland). Lithos 86, 260–280.

Ramadhan, Q.S., Sianipar, J.Y., Pratopo, A.K., 2016. Volcanostratigraphic approach for evaluation of geothermal potential in Galunggung volcano. IOP Conf. Ser.: Earth Environ. Sci. 42, 012028.

Renjith, M.L., 2014. Micro-textures in plagioclase from 1994–1995 eruption, Barren Island Volcano: Evidence of dynamic magma plumbing system in the Andaman subduction zone. Geosci. Front. 5, 113–126.

Sendjaja, Y.A., Kimura, J.I., Sunardi, E., 2009. Across-arc geochemical variation of Quaternary lavas in West Java, Indonesia: Mass-balance elucidation using arc basalt simulator model. Isl. Arc 18, 201–224.

Soeria-Atmadja, R., Maury, R.C., Bellon, H., Pringgoprawiro, H., Polve, M., Priadi, B., 1994. Tertiary magmatic belts in Java. J. Southeast Asian Earth Sci. 9, 13–27.

Tilling, R.I., 1989. Volcanic hazards and their mitigation: Progress and problems. Rev. Geophys. 27, 237–269.

Toramaru, A., Noguchi, S., Oyoshihara, S., Tsune, A., 2008. MND (microlite number density) water exsolution rate meter. J. Volcanol. Geotherm. Res. 175, 156–167.

Tsai, Y.W., Song, S.R., Chen, H.F., Li, S.F., Lo, C.H., Lo, W., Tsao, S., 2010. Volcanic stratigraphy and potential hazards of the Chihsingshan volcano subgroup in the Tatun Volcano Group, northern Taiwan. Terr. Atmos. Ocean. Sci. 21, 587–598.

Tsuchiyama, A., 1985. Dissolution kinetics of plagioclase in the melt of the system diopside-albite-anorthite, and origin of dusty plagioclase in andesites. Contrib. Mineral. Petrol. 89, 1–16.

van Bemmelen, R.W., 1949. The Geology of Indonesia. General Geology of Indonesia and Adjacent Archipelagos. Government Printing Office, The Hague.

van Bemmelen, R.W., 1970. The Geology of Indonesia. Nijhoff, The Hague.

Vance, J.A., 1962. Zoning in igneous plagioclase: Normal and oscillatory zoning. Am. J. Sci. 260, 746–760.

Vance, J.A., 1969. On synneusis. Contrib. Mineral. Petrol. 24, 7–29.

Vernon, R.H., 2008. A Practical Guide to Rock Microstructure. Cambridge University Press, Cambridge.

Viccaro, M., Giacomoni, P.P., Ferlito, C., Cristofolini, R., 2010. Dynamics of magma supply at Mt. Etna volcano (Southern Italy) as revealed by textural and compositional features of plagioclase phenocrysts. Lithos 116, 77–91.

Viccaro, M., Giuffrida, M., Nicotra, E., Ozerov, A.Y., 2012. Magma storage, ascent and recharge history prior to the 1991 eruption at Avachinsky Volcano, Kamchatka, Russia: Inferences on the plumbing system geometry. Lithos 140–141, 11–24.

Winter, J.D., 2001. An Introduction to Igneous and Metamorphic Petrology. Prentice Hall, New Jersey.